Chemical Kinetics Study of the Sol−Gel Processing of GeS_2

Vesna Stanić,* Alain C. Pierre, and Thomas H. Etsell

Department of Chemical and Materials Engineering, The University of Alberta, Edmonton, AB T6G 2G6, Canada

Randy J. Mikula

CANMET Western Research Centre, Devon, AB T0C 1E0, Canada

Received: January 11, 2001

A chemical kinetics study of the functional groups $-OC_2H_5$, SH^-, and S^{2-} was carried out for the sol−gel processing of GeS_2 from hydrogen sulfide and germanium ethoxide in toluene. A mass balance of the reaction components was monitored by potentiometric titrations of SH^- and S^{2-} with the Ag/Ag_2S ion-selective electrode. The study was performed for different concentrations of precursors at different molar ratios and temperatures. The results indicate that the proposed reaction mechanism was simplified under appropriate reaction conditions. Experimentally determined rate constants of thiolysis and condensations demonstrate that thiolysis is slow and that condensations are fast steps, regardless of reaction conditions (concentration, rate, and temperature). A study of the temperature effect on the reaction rate constants shows that they increase with temperature in accord with both Arrhenius law and transition-state theory. Activation energies, E_a, and activation parameters $\Delta S^{\ddagger}$, $\Delta H^{\ddagger}$, and $\Delta G^{\ddagger}$ were determined for thiolysis and condensation reactions.

Introduction

Sol−gel processing is a promising method for the preparation of advanced ceramics such as metal sulfides. The reaction product of the sol−gel synthesis could be either colloidal powder or gel. One of the advantages of this method is the ability to control the microstructure of the final product by controlling chemical reaction parameters. It was demonstrated that modification of the reaction conditions can significantly affect the structure of the sol−gel product.[1] The connection between the sol−gel process kinetics and the sol−gel product microstructure can be illustrated by the following sequence:[2]

solvolysis (hydrolysis, thiolysis) →
condensation → nucleation → growth → aggregation

Therefore, the chemical reactions, solvolysis and condensation, are ultimately succeeded by phase transformation, nucleation, growth and aggregation during sol−gel process providing the connection between reaction chemistry and product structure.

In the sol−gel literature publications concerning the process of hydrolysis and condensation of silicon alkoxides exist. These investigations show that under well-defined conditions detailed statements about reaction mechanisms can be made.

One of the earliest attempts to study chemical kinetics of sol−gel process was made by Strelko.[3] He made a theoretical explanation of the condensation mechanism of silicic acid on the basis of donor−acceptor properties. McNeilet et al.[4] determined the apparent hydrolysis reaction constants of tris-(2-methoxyethoxy)-phenyl silane at different temperatures. The importance of this work is that for the first time reaction of the silica precursors was studied in a purely aqueous medium and that reaction activation parameters were determined.

Assink and Kay[5] introduced proton nuclear magnetic resonance (^1H NMR) spectroscopy in investigations of both the temporal and chemical nature of sol−gel reactions. They studied the sol−gel kinetics of the functional groups in the acid-catalyzed reaction of $Si(OCH_3)_4$ and H_2O.[6] Their work continued to a theoretical kinetic formalism which specifically treated the evolution of various transient groups at a silicon atom undergoing hydrolysis and condensation.[6−9]

The kinetics of $Si(OC_2H_5)_4$ sol−gel condensation using ^{29}Si NMR spectroscopy was studied by Pouxviel et al.[10] They used mathematical simulations of the reaction mechanism in order to predict the size of the colloidal particles formed.[11]

To explore the possibility of reducing gelation time without affecting the characteristics of the resulting gel, Artaki et al.[12] investigated the influence of pressure on the condensation kinetics of $Si(OCH_3)_4$ in an acid-catalyzed reaction.

However, Ro et al.[13] examined the acid catalytic reactions of $Si(OC_2H_5)_4$ by measuring the temperature profile during hydrolysis.

A new method, cylindrical attenuated total reflectance infrared spectroscopy, for monitoring in-situ kinetics of the sol−gel processing acidic $Si(OC_2H_5)_4$ and $Al(NO_3)_3{\cdot}9H_2O$ in ethanol−water solutions was employed for the first time by Kline et al.[14] They determined reaction rate constants at various temperatures and did computer modeling on the experimental results $C = f(t)$.[15]

The effect of various base catalysts on the reaction kinetics of $Si(OC_2H_5)_4$ in ethanol−water solutions was studied by Sanchez et al.[16] They obtained apparent activation energies from a simplified kinetics model.

Liu et al.[17] reported results of ^1H and ^{13}C NMR characterizations performed on a system of methyl-threemetoxysilane as the precursor and ethanol as the solvent. Their results revealed complicated structures of the reaction intermediates.

This brief review of research on the kinetics of the sol−gel processing of silica illustrates important achievements in the investigation of the most frequently studied sol−gel prepared material, silica gel from alkoxide precursor.

10.1021/jp010138j CCC: $20.00
Published on Web 06/05/2001

TABLE 1: The Concentrations of Reactants and Their Molar Ratio Used for the Preparation of the Chemical Kinetics Study

alkoxide	$[Ge(OR)_4]_o$ (M)	H_2S (M)	$[Ge(OR)_4]_o/[H_2S]_o$
$Ge(OEt)_4$	0.044	0.400	1:9
$Ge(OEt)_4$	0.264	0.220	1.2:1

This work represents a first attempt in the chemical kinetics study of the sol−gel processing of GeS_2 from germanium alkoxide and hydrogen sulfide in toluene. The reaction mechanism was studied under reaction conditions that enabled simplification of the proposed reaction scheme and mathematical expressions for computation of the reaction rate constants. The reaction rate constants of thiolysis and condensations were determined as the functions of temperatures, from 30 to 50 °C, to derive activation energies and activation parameters.

Experimental Section

A. Materials. Germanium ethoxide, $Ge(OC_2H_5)_4$, manufactured by Aldrich Co. (99.99%, per metal basis), and hydrogen sulfide (Linde Canada, 99.6% of H_2S) were used as precursors. Toluene (Fisher Scientific, HPLC grade) was dried prior to use by refluxing over Na metal. To get pure toluene for the experiments, it was distilled after refluxing.

B. Kinetics Procedure. The reaction mixtures were prepared in the following way. First, toluene was saturated with the H_2S gas for several hours. The concentration of the solution obtained was determined by potentiometric titration.[18] The proper volume of this solution was placed in a 50 mL reaction glass vessel by pipetting and diluted to the desired H_2S concentration with toluene.

After this, the reaction vessel was capped with a rubber septum and placed in a constant-temperature bath (HAAK 20), filled with ethylene glycol. The H_2S solution was thermostated for ∼0.5 h prior to addition of germanium ethoxide. Desired volumes of germanium ethoxide were added via a syringe into the H_2S solutions and mixed by shaking. The reaction mixture concentrations are listed in Table 1.

The reaction mixtures were thermally equilibrated (±0.1 °C) for 0.5 or 1 h. At proper intervals (0.5 or 1 h), 1-mL aliquots were removed by syringe from the mixture. They were injected into 100-mL flasks containing 25 mL of toluene, agitated, and cooled to ∼ −95 °C. Unreacted H_2S was quickly purged from the flasks by nitrogen. Then, the samples were analyzed by potentiometric titration with the Ag/Ag_2S ion selective electrode.

The temperature effect on the reaction constants was studied at 30, 40, 45, and 50 °C.

C. Analysis. Quantitative chemical analysis of the kinetic samples was done by potentiometric titration of mercaptide (≡GeSH) and sulfide (≡GeSGe≡) evolved during reaction. The detailed procedure was previously reported.[18] These concentrations were used for all mass-balance calculations.

Softwear Enzfiter−Version 1.05 EGA (Elsevier Biosoft, Cambridge U.K, 1987) was used for plotting linear graphs by linear regression analysis.

Theoretical Considerations

Melling[19] proposed the mechanism of $Ge(OEt)_4$ and H_2S reaction, analogous to that of $Si(OEt)_4$ and H_2O, that involved three steps per S_N2 (bimolecular nucleophilic substitution):

I step: thiolysis

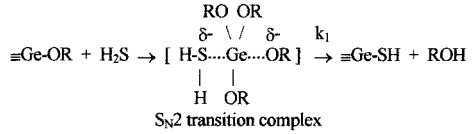

(1)

II step: H_2S forming condensations

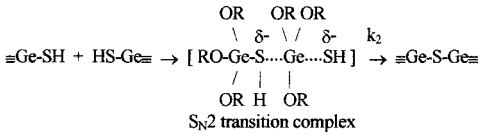

(2)

III step: ROH forming condensation

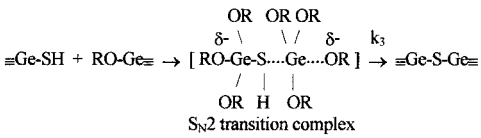

(3)

where R is the ethyl group, k_1 is the thiolysis rate constant, k_2 is the hydrogen sulfide-forming condensation rate constant, and k_3 is the alcohol-forming condensation rate constant. This is a simplified scheme of a very complex reaction mechanism consisting of a series of consecutive, parallel, and reverse reactions whose intermediate products can have structures as complicated as $GeS_x(SH)_y(OR)_{4-z}$, where $2x + y + z = 4$. The overall reaction from eqs 1−3 is

$$\equiv Ge(OR) + \equiv Ge(SH) = \equiv GeSGe\equiv + ROH \qquad (4)$$

Therefore, germanium alkoxide, germanium mercaptide, germanium sulfide, and the corresponding alcohol are present at equilibrium. All these compounds were identified in the dried gels by infrared spectroscopy.[20]

Assuming that reaction rate constants are independent of the number of substituted functional groups per Ge atom during thiolysis (−OR) and condensations (−SH), the reaction rate equations can be expressed from eq (1−3):

$$-\frac{d[A]}{dt} = k_1[A][B] + k_3[A][C] \qquad (5)$$

$$-\frac{d[B]}{dt} = k_1[A][B] - k_2[C]^2 \qquad (6)$$

$$-\frac{d[C]}{dt} = k_1[A][B] - k_2[C]^2 - k_3[A][C] \qquad (7)$$

$$-\frac{d[M]}{dt} = k_2[C]^2 + k_3[A][C] \qquad (8)$$

$$-\frac{d[D]}{dt} = k_1[A][B] + k_3[A][C] \qquad (9)$$

where [A] = [≡GeOR], [B] = [H_2S], [C] = [≡GeSH], [D] = [ROH], and [M] = [≡Ge−S−Ge≡] are the reactant and product concentrations in mol/L present in the reaction mixture at time t.

From the reaction stoichiometry and mass conservation, relationships among concentrations of reactants and products can be given:

$$[A]_o = 4[Ge(OR)_4]$$

where $[A]_o$ is the initial concentration of ethoxy groups (OR) from which the concentration of substituted ethoxy groups, $[X]_A$, is

$$[X]_A = [A]_o - [A]$$

and reacted hydrogen sulfide, $[X]_B$, is

$$[X]_B = [B]_o - [B]$$

From the mass concentration law,

$$[X]_A = [C] + 2[M]$$

$$[X]_B = [C] + [M]$$

the concentration of the reacted ethoxy groups, $[X]_A$, or hydrogen sulfide, $[X]_B$, are equal to the sum of concentrations of mercaptide [C] and sulfide [M]. In early stages of thiolysis, it could be assumed that the reaction occurs with no interference of the condensation reaction. Therefore,

$$[X]_A \approx [X]_B = [X]$$

and

$$[X] = [C] + [M]$$

represents the concentration of unreacted ethoxy groups. In addition, the concentration of the formed alcohol is

$$[D] = [X] = [A]_o - [A]$$

Hence, by measuring the concentrations of evolved mercaptide and sulfide it is possible to monitor how the concentrations of all other products and reactants change with time.

It is speculated that the proposed reaction mechanism (eqs 1−3) can also involve the reverse reaction steps. Therefore, the agreement of the experimentally determined rate law and the proposed mechanism will evidence the actual reaction mechanism.

In the suggested reaction scheme, germanium mercaptide is an intermediate product. It reacts further by two competitive parallel reactions, eqs 2 and 4. The kinetics of this complex reaction system can conveniently be approximated, provided the intermediate ≡GeSH is either equilibrated or transient.[21] According to approximation competition for an equilibrated intermediate (CEI),[21] the concentration of the intermediate (≡GeSH) will equilibrate under the assumption that thiolysis is a fast and reversible reaction and thus,

$$[C] = \frac{k_1}{k_{-1}} \cdot \frac{[A][B]}{[D]} \tag{10}$$

This approximation is valid only if substitution in the kinetic eqs 5−9 gives agreement with the experimental results.

However, the approximation competition for the transient intermediate (CTI)[21] is applicable if the rate constants for the competition condensation reactions, k_2 and k_3, are much greater than the thiolysis rate constant. In such a case, the concentration of the intermediate [C] is much less than [A]. Therefore, from the approximation

$$\frac{d[C]}{dt} \approx 0 \tag{11}$$

and eq 7 the concentration of the intermediate, [C], can be calculated.

If thiolysis is a reversible reaction, then

$$k_{-1}[D] \gg k_2[C] + k_3[A] \tag{12}$$

meaning the intermediate germanium mercaptide is equilibrated as well as transient and then both approximations are applicable. However, if

$$k_{-1}[D] \ll k_2[C] + k_3[A] \tag{13}$$

the thiolysis is virtually irreversible.

The experiments may confirm the reaction scheme and give solutions to which of the conditions lead to certain approximations and thus simplify interpretation of the kinetic data.

Even after these approximations, CTI or CEI, the multiple term differential eqs 5−9 are difficult mathematical problems for which to obtain exact solutions of the rate constants. One of the methods that enables simplification of the mathematical expressions for computation of the reaction rate constants is the method of concentration−time integrals.[21] For example, if the reaction occurs only per two steps described by eq 1 and 3, then the differential rate eq 5 is

$$-\frac{d[A]}{dt} = k_1[A][B] + k_3[A][C] \tag{14}$$

After rearrangement and integration it becomes

$$\ln\frac{[A]_0}{[A]} = k_1 \int_0^t [B]\, dt + k_3 \int_0^t [C]\, dt \tag{15}$$

or

$$\frac{\ln\frac{[A]_0}{[A]}}{\int_0^t [B]\, dt} = k_1 + k_3 \frac{\int_0^t [C]\, dt}{\int_0^t [B]\, dt} \tag{16}$$

From experimental data of [C] and [M], the concentrations [A] and [B] can be calculated as functions of time and then used for obtaining the concentration integrals. Equation 16 suggests a linear plot whose intercept is k_1 and slope is k_3.

The other mathematical method which permits calculation of the rate constants is a differential method.[22] The procedure considers a single run where the measured reaction rate at different reaction times corresponds to the reactant (or product) concentration. For example, if it is assumed that condensation occurs only per the alcohol-forming condensation reaction, eq 3, then the reaction rate of sulfide formation is

$$\frac{d[M]}{dt} = k_3[A][C] \tag{17}$$

If the reaction rate is measured in the early stages of the reaction, the following assumption can be made:

$$[A] \gg [C] + [M]$$

and therefore,

$$[A] \approx [A]_o$$

Thus, a plot of eq 17 is linear with slope equal $k_3[A]_o$ from which the reaction rate constant can be calculated.

If it is possible to make a supposition that only thiolysis (eq 1) occurs with no condensation reaction interference, as the second-order reaction, then the differential rate eq 5 becomes

$$-\frac{d[A]}{dt} = k_1[A][B] \tag{18}$$

and after integration it is

$$\frac{1}{[B]_o - [A]_o} \ln\frac{[A]_o[B]}{[B]_o[A]} = k_1 t \tag{19}$$

Experimental data will give a linear plot of eq 19 if the assumption is correct. Additional simplification in the integration of eq 18 is possible to make if one of the reactants, for instance (B), is in a great excess, considered as constant in the observed reaction interval. This assumption provides pseudo-first-order kinetics.[21] Hence, the integrated form of eq 18 will be

$$\ln\frac{[A]}{[A]_o} = k_{app}' t \tag{20}$$

The constant $k_{app}' = k_1[B]_o$ can be determined from the slope of the linear graph, if the experimental results coincide with the pseudo-first-order assumption.

The temperature dependence of the rate constants of thiolysis and condensations reactions were studied using two different equations. One of them was the Arrhenius relation[23] in which frequency factor A is taken as independent of temperature. The other one is the absolute reaction rate theory relation (or the transition-state theory)[23] where the preexponential parameter shows a first power temperature dependence.

Results

A. Kinetic Data. Samples taken from reaction mixture at different times after purging the unreacted H_2S were analyzed by potentiometric titration. Potentiometric curves $E = f(V_{add.titr.})$ were plotted for each sample. From the equivalence points of the potentiometric curves, the concentrations of S^{2-} (M) and SH^- (C) evolved during the reaction were determined.[18]

B. Reaction Mixtures Containing $[Ge(OEt)_4]_o$ and $[H_2S]_o$ in Molar Ratio 1:9. The sol−gel reaction of germanium ethoxide and hydrogen sulfide in a molar concentration ratio 1:9 was performed at four different temperatures 30, 40, 45 and 50 °C. The Tyndall effect appeared after ∼ 9.5 h, while all samples gelled within 12−14 h from the beginning of the reaction.

Typical concentration−time data for reactant ethoxide (A), intermediate mercaptide (C), and product sulfide (M) are plotted in Figure 1. There is a concentration−time delay, induction period, before sulfide (M) appeared in significant concentrations, as seen on the curve $[M] = f(t)$. The extent of the induction period varies with temperature. It was the shortest at 50 °C, 5 h, increased to 6 h at 45 and 40 °C, and even to 9 h at 30 °C. The concentration of germanium mercaptide [C] measured at the end of the induction periods was $\approx 1.29 \times 10^{-3}$ M at all temperatures.

There are two distinguishable linear parts on plots $-\ln([A]/[A]_o)$ versus time. In Figure 2 the first linear parts of these curves

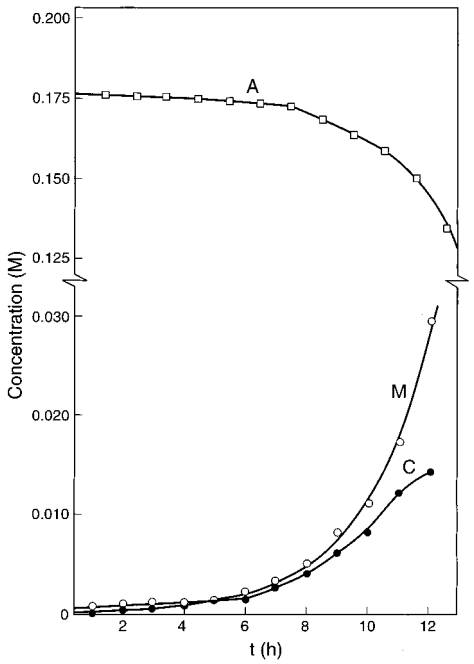

Figure 1. The reactant/product concentration as a function of time for the sol−gel reaction when $[Ge(OEt)_4]_o/[H_2S]_o$ is 1:9: M − sulfide (≡GeSGe≡); C− mercaptide (≡GeSH); A − ethoxy group (≡GeOEt).

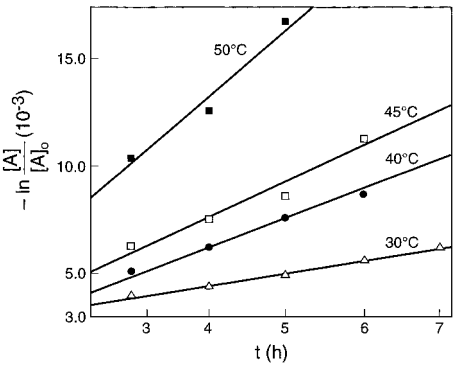

Figure 2. Plots $-\ln([A]/[A]_o)$ vs time for various temperatures when $[Ge(OEt)_4]_o/[H_2S]$ is 1:9.

TABLE 2: The Thiolysis (k_1) and the Condensation (k_3) Rate Constants Obtained from Apparent Values k_{app}' and k_{app}''', Respectively, at Different Temperatures for the Sol−Gel Process if $[Ge(OR)_4]/[H_2]$ is 1:9

temperature (°C)	k_{app}' $\times 10^{-7}(s^{-1})$	k_1 $\times 10^{-7}(M\cdot s)^{-1}$	k_{app}''' $\times 10^{-4}(M\cdot s)^{-1}$	k_3 $\times 10^{-4}(M\cdot s)^{-1}$
30	1.542	3.856	0.225	1.278
40	3.922	9.806	0.512	2.911
45	5.625	14.061	0.836	4.747
50	7.972	19.931	1.298	7.374

for various temperatures are shown. The length of this linear part overlaps with the induction period. Its linearity indicates that the thiolysis is of the first order with the respect to the concentration of ethoxide groups [A] in this reaction period. Thus, it was assumed that thiolysis was the pseudo-first-order reaction in regards to [A]. The slopes of the straight lines $-\ln([A]/[A]_o) = f(t)$ are assigned to the apparent thiolysis rate constants $k_{app}' = k_1 B_o$. The apparent constant k_{app}' and calculated k_1 constants are listed in Table 2.

To determine the condensation rate constants, plots $\Delta M/\Delta t$ as ordinate against [C] as abscissa were made for various temperatures (Figure 3). The reaction rate of sulfide appearance, $\Delta M/\Delta t$, was calculated for sulfide concentrations in the reaction period which coincides with the second linear part of the graph

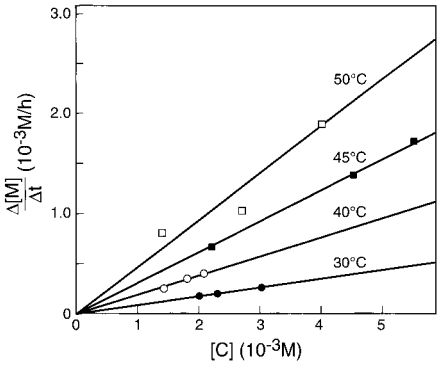

Figure 3. Plots reaction rate of sulfide formation, $\Delta[M]/\Delta t$, as the functions of mercaptide concentrations [C] for various temperatures for the sol−gel process when $[Ge(OEt)_4]_o/[H_2]_o$ ratio is 1:9.

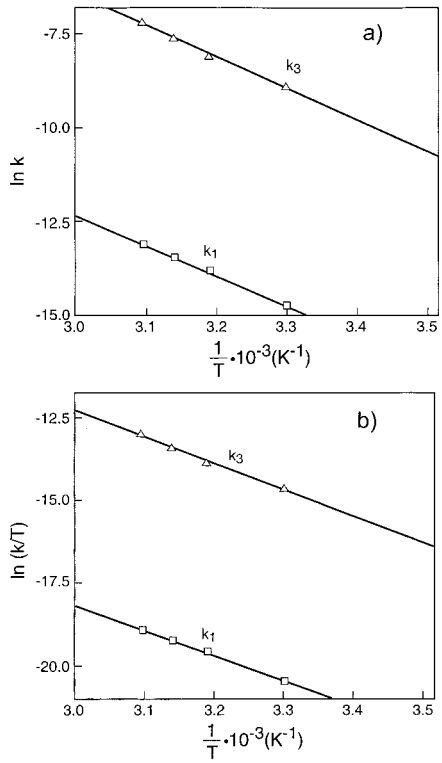

Figure 4. Influence of the reaction temperature on the thiolysis (k_1) and condensation (k_3) rate constants: (a) Arrhenius plot, ln k vs ($1/T$); (b) transition-state theory plot, ln(k/T) vs ($1/T$), for the sol−gel process if $[Ge(OEt)_4]/[H_2S]$ is 1:9.

$-\ln([A]/[A]_o) = f(t)$. The slope of this plot is assigned to the apparent alcohol-forming condensation rate constant $k_{app}''' = k_3[A]_o$. The apparent constants k_{app}''' and calculated values of k_3 are shown in Table 2. Values of the same order were obtained for k_3 when the concentration−time integral method was used.

The functional relationship for the reaction rates k_1 and k_3 with temperature was determined using the Arrhenius plots, ln k vs $1/T$, and the transition-state theory plots, ln(k/T) vs $1/T$. They are shown in Figure 4a and b, respectively. From the slopes of the lines in Figure 4a, the activation energies of thiolysis and condensation are calculated and from the intercepts the frequency factors. The enthalpies $\Delta H^{\ddagger}$ of thiolysis and condensation reactions were calculated from the slopes of the graphs in Figure 4b. The intercepts were used to calculate the activation entropies $\Delta S^{\ddagger}$ of both reactions. From these activation parameters the free energies for the transition state of thiolysis (TS1) and condensation (TS2), were obtained from the Gibbs-Helmholtz equation[23] for the middle of the studied temperature range, $T = 314.25$ K.

TABLE 3: Activation Energies, Frequency Factors, and Activation Parameters of the Sol−Gel Processing Reactions if $[Ge(OEt)_4]/[H_2S]$ is 1:9

reaction	E_a (kJ/mol)	A $(M\cdot s)^{-1}$	$\Delta S^{\ddagger}$ (J/mol K)	$\Delta H^{\ddagger}$ (kJ/mol)	$\Delta G^{\ddagger}$ (kJ/mol)
thiolysis (k_1)	66.886	1.3×10^5	−155.52	64.301	113.74
condensation (k_3)	70.877	2.0×10^8	−94.52	68.295	98.00

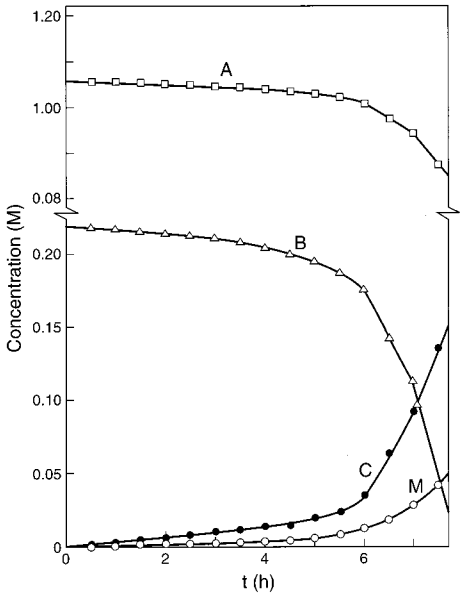

Figure 5. The mass balance as a function of time for the sol−gel process if $[Ge(OEt)_4]_o/[H_2S]$ is 1.2:1. The concentrations of sulfide M and mercaptide C were determined experimentally, while the concentrations of ethoxy group A and hydrogen sulfide B were calculated.

The activation energies E_a, frequency factors A, and activation parameters are listed in Table 3.

The sol−gel reaction enthalpy ΔH was calculated from the enthalpies of activations for thiolysis $\Delta H_t^{\ddagger}$ and condensation $\Delta H_c^{\ddagger}$,

$$\Delta H = \Delta H_t^{\ddagger} - \Delta H_c^{\ddagger} = 4\text{kJ/mol}$$

C. Reaction Mixtures Containing $[Ge(OEt)_4]_o$ and $[H_2S]_o$ in Molar Ratio 1.2:1. Sol−gel processing of germanium sulfide from germanium ethoxide and hydrogen sulfide in an initial molar ratio of 1.2:1 was performed at various temperatures: 30, 40, 45, and 50 °C. Tyndall effect appearing after ∼10 h from the reaction start was succeeded by gelation within the next 2 h.

The material balance graph shown in Figure 5 is typical for all reactions studied at different temperatures. The curve representing the sulfide concentration as a function of time, $[M]=f(t)$, exhibits an induction period similar to that presented in Figure 1. The induction periods ended after 2.5 h at 50 °C and after 3.5 h at lower temperatures, 45, 40, and 30 °C. The concentrations of the intermediate mercaptide were different: 2.20×10^{-3} M at 30 °C, 2.63×10^{-3} M at 40 °C, 8.1×10^{-3} M at 45 °C, and 8.69×10^{-3} M at 50 °C.

In Figure 6, plots of $-\ln([A]/[A]_o)$ and $-\ln([B]/[B]_o)$ versus time are represented. A linear part on each curve coincides with the induction period. For this reaction period, a plot of $\{1/([B]_o - [A]_o)\}\ln([A]_o[B]/[A][B]_o)$ against time was made. Graphs

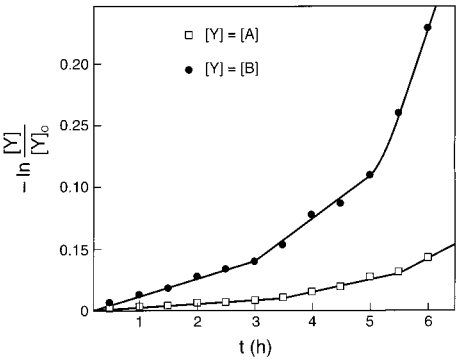

Figure 6. Plot $-\ln([Y]/[Y]_o)$ as a function of time if Y is (a) ethoxide group concentration [A]; (b) hydrogen sulfide concentration [B]. The reaction was performed at 50 °C with $[Ge(OEt)_4]_o/[H_2S]$ ratio 1.2:1.

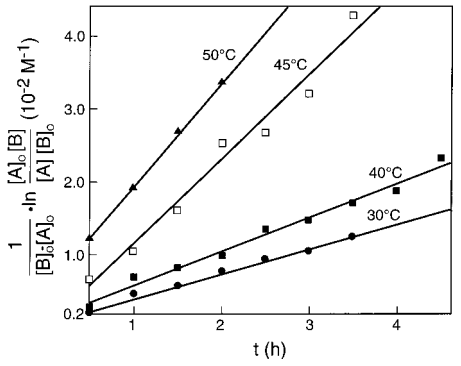

Figure 7. Plots $\frac{1}{[B]_o - [A]_o}\ln\frac{[A]_o[B]}{[A][B]_o}$ as functions of time made for the induction period, at different reaction temperatures and $[Ge(OEt)_4]/[H_2]$ ratio 1.2:1.

TABLE 4: Thiolysis Rate Constant Obtained for the Sol−Gel Processing If $[Ge(OEt)_4]/[H_2S]$ is 1.2:1

temperature (°C)	$k_1 \times 10^{-6}$ $(M\cdot s)^{-1}$
30	0.942
40	1.306
45	3.208
50	3.935

obtained for the reactions carried out at different temperatures are shown in Figure 7. The slopes of these graphs are assigned to the thiolysis rate constants, listed in Table 4.

To determine the influence of temperature on the thiolysis rate constant, an Arrhenius plot, ln k vs $1/T$, and a transition-state theory plot, $\ln(k/T)$ vs $1/T$, were made. From the slope of the line ln k vs $1/T$ an activation energy $E_a = 61.19$ kJ/mol was calculated. The intercept of the graph $\ln A = 10.3$ was used to calculate the frequency factor $A = 3 \times 10^4$. Activation parameters obtained from the plot $\ln(k/T)$ vs $1/T$ are as follows: $\Delta H^{\ddagger} = 57.47$ kJ/mol, $\Delta S^{\ddagger} = -170.70$ J mol^{-1} $K^{-1}$and $\Delta G^{\ddagger} = 111.11$ kJ/mol, for the middle of the used temperature interval, $T = 314.25$ K.

Discussion

A. Reaction Mixtures Containing $[Ge(OEt)_4]_o$ and $[H_2S]_o$ in Molar Ratio 1:9. The induction period, exhibited in Figure 1, indicates that reaction occurs slowly. During this time there was a buildup toward a small but critical concentration of the intermediate, germanium mercaptide. This critical concentration was found to be $\sim 1.29 \times 10^{-3}$ M, regardless of the reaction temperature. However, the temperature influenced the length of the induction period. Once the critical concentration was achieved, the reaction rate suddenly increased, indicating that another much faster reaction began. From this result it was assumed that the reaction rate of the ethoxy group depletion, eq 5, could be simplified during the induction period to

$$-\frac{d[A]}{dt} = k_1[A][B] \tag{21}$$

This assumption is a consequence of a very low concentration of intermediate C in comparison to the reactant concentrations. Thus, all expressions in eq 5 containing [C] can be neglected. Therefore, it could be concluded that, during the induction period, thiolysis occurs with no interference from the condensation reactions.

The linearity of graphs $-\ln([A]/[A]_o)$ vs time during the induction period indicates that the reaction was first order in regards to the concentration of the ethoxy group. Moreover, since the concentration of hydrogen sulfide was in excess and almost constant during the induction period, it was suspected that the reaction occurred as a pseudo-first order. Consequently, the integrated form of eq 21 is

$$\ln\frac{[A]}{[A]_o} = k_{app}'t \tag{22}$$

where

$$k_{app}' = k_1[B]_o \tag{23}$$

is the apparent first-order rate constant obtained from the slope of the plot $-\ln[A]/[A]_o$ vs time. From these experimentally determined rate constants and initial concentration of hydrogen sulfide $[B]_o$, the thiolysis rate constants were calculated. As a second-order rate constant, they indicate that thiolysis is a bimolecular reaction.

After the induction period, the reaction became too complicated. It is possible that two condensation reactions started to proceed more extensively. The experimental results for [M] and [C] when plotted as $\Delta[M]/\Delta t$ versus [C] (Figure 3) indicate that dominant condensation reaction is the alcohol-forming condensation (k_3). The linearity of these plots unambiguously confirms that eq 8 is valid in the simplified form:

$$-\frac{d[M]}{dt} = k_3[A][C] \tag{24}$$

and that

$$k_3[A] \approx k_3[A]_o \approx \text{constant} \tag{25}$$

The approximation in eq 25 is reasonable for this initial period of the condensation reaction when the concentration of intermediate C is still very low, i.e., $[C] \ll [A]$. Therefore, the reaction rate of sulfide formation defined by eq 24 represents the initial rate of the sulfide condensation reaction k_3.

The absence of the hydrogen sulfide-forming condensation in this early reaction stage can be explained by the very low [C], if the condensation rate constants k_2 and k_3 are of the same order. When this small value is squared it becomes negligible. Accordingly, there is a critical mercaptide concentration which triggers the hydrogen sulfide-forming condensation probably later on during the sol−gel process. However, it is also possible that $k_2 \ll k_3$ and that germanium sulfide is mainly a product of the alcohol-forming condensation regardless of the concentration of intermediate C.

From these experimental results, a simplified reaction scheme can be proposed for the reaction conditions imposed:

$$\equiv\text{Ge}-\text{OEt} + \text{H}_2\text{S} \xrightarrow{k_1} \equiv\text{Ge}-\text{SH} + \text{EtOH} \qquad (26)$$

$$\equiv\text{Ge}-\text{OEt} + \text{HS}-\text{Ge}\equiv \xrightarrow{k_3} \equiv\text{Ge}-\text{S}-\text{Ge}\equiv + \text{EtOH} \qquad (27)$$

Hence, the rate law which defines the proposed reaction mechanism is

$$-\frac{\text{d[A]}}{\text{d}t} = k_1[\text{A}][\text{B}] + k_3[\text{A}][\text{C}] \qquad (28)$$

$$\frac{\text{d[C]}}{\text{d}t} = k_1[\text{A}][\text{B}] - k_3[\text{A}][\text{C}] \qquad (29)$$

$$\frac{\text{d[M]}}{\text{d}t} = k_3[\text{A}][\text{C}] \qquad (30)$$

The experimentally determined thiolysis and condensation rate constants at different temperatures exhibit good agreement with the Arrhenius equation demonstrated in Figure 4a. The activation energies of thiolysis and condensation (Table 3) determined from the slopes of these graphs have values typical for the bimolecular nuclear substitution.[24] Therefore, the functional relationship of the rate constants and temperature is represented as follows:

$$\ln[k_1(\text{M}\cdot\text{s})^{-1}] = -(8845\ \text{K})/T + 11.8 \qquad (31)$$

$$\ln[k_3(\text{M}\cdot\text{s})^{-1}] = -(8525\ \text{K})/T + 19.2 \qquad (32)$$

For bimolecular reactions involving relatively simple molecules, the frequency factor A generally has values of order 10^9 to 10^{11} $(M\cdot\text{s})^{-1}$.[25] However, for the thiolysis reaction it was 1.3×10^5 and condensation 2×10^8, indicating reactions between complex molecules.[25] Transition-state theory provides the clear explanations for such values of frequency factor A. The activation entropy $\Delta S^{\ddagger}$ is a measure of disorder in the activated complex. The decrease in entropy reflects the decrease in the activated complex disorder caused by loss of motional mode of molecules in the transition state. For bimolecular reaction, such as S_N2, two reactant particles are converted to a single activation complex in a transition state. The loss of the molecular rotational and translational degrees of freedom in the transition state causes a decrease of corresponding entropies. The resulting total entropy changes $\Delta S^{\ddagger}$ during thiolysis and condensation are negative, typical for an associative mechanism of ligand substitution by S_N2.[25]

From the results in Table 3 it is obvious that the activation complex formed during thiolysis is a more ordered structure than that formed during condensation. This difference in entropy could be explained by a steric effect. Increased steric crowding during condensation increased the entropy of TS2. However, steric crowding increases the activation energy of Ge−S−Ge formation as seen from $\Delta H^{\ddagger}$ and E_a (Table 3).

Using data from Table 3 for standard activation free energies $\Delta G^{\ddagger}$ for the transition state of thiolysis (TS1) and condensation (TS2), the free energy vs reaction coordinate diagram was sketched in Figure 9. The transition states correspond to the maxima in the diagram. There is a free energy local minimum between them assigned to the intermediate germanium mercaptide. The first maximum is apparently higher than the second one. From this result and from the reaction rate constants k_1 and k_3, it is evident that the rate-limiting step for this sol−gel reaction is thiolysis.

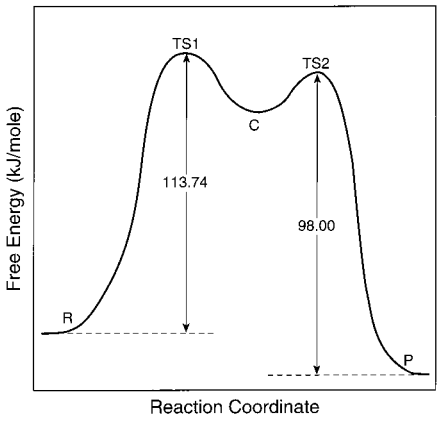

Figure 8. Free energy−reaction coordinate diagram for the sol−gel processing of GeS_2 when $[Ge(OEt)_4]_o/[H_2]_o$ is 1:9.

B. Reaction Mixtures Containing $[Ge(OEt)_4]_o$ and $[H_2S]_o$ in Ratio 1.2:1. Initial mixtures for the chemical kinetics investigation were prepared with H_2S in a sub stoichiometric amount (<4).

The concentration−time plots indicate the presence of an induction period. During this period the reaction was second order as demonstrated with the plots in Figure 7. According to this, it was assumed that during the induction period thiolysis occurred with no condensation interference.

Moreover, the concentration−time curves for this reaction are similar to those obtained for the pseudo-first order reaction (Figure 1). That is, after the induction period, a much faster reaction started when the intermediate mercaptide reached the critical concentration. Further, none of the applied mathematical methods for the condensation rate constant calculations gave a reasonable match with the experimental results. Therefore, it is suspected that both hydrogen sulfide- and alcohol-forming condensations simultaneously started after the induction period. Consequently, the proposed complex reaction mechanism, given by eqs 1−3, is applicable for the sol−gel reaction with low H_2S content. For these conditions, the proposed rate law is

$$-\frac{\text{d[A]}}{\text{d}t} = k_1[\text{A}][\text{B}] + k_3[\text{A}][\text{C}] \qquad (33)$$

$$\frac{\text{d[C]}}{\text{d}t} = k_1[\text{A}][\text{B}] - k_2[\text{C}]^2 - k_3[\text{A}][\text{C}] \qquad (34)$$

$$\frac{\text{d[M]}}{\text{d}t} = k_2[\text{C}]^2 + k_3[\text{A}][\text{C}] \qquad (35)$$

The best fit straight line for the thiolysis rate constant dependence on temperature is represented by

$$\ln k_1(\text{M}\cdot\text{s})^{-1} = -(7360\ \text{K})/T + 10.3 \qquad (36)$$

The activation energy E_a and the activation enthalpy $\Delta H^{\ddagger}$ of thiolysis obtained for these reaction conditions are very similar to those for the reaction with H_2S in excess (Table 3). This result is reasonable since in both reactions, the same reactants, ≡GeOEt and H_2S, and same products, ≡GeSH and EtOH, are involved. Although the reaction conditions are different, the same chemical bonds are broken and formed during thiolysis. Moreover, the activation entropy $\Delta S^{\ddagger}$ that is negative, indicates that thiolysis occurs by an associative mechanism of two molecules (S_N2). The numerical value of $\Delta S^{\ddagger}$ is lower than that

for the pseudo-first-order reaction (Table 3), increasing the thiolysis rate constant ~2 times.

Therefore, it could be suggested that low H_2S concentration caused the simultaneous occurrence of both condensation reactions due to a significant increase in the intermediate mercaptide concentration. However, it did not change the reaction type. All of them followed the S_N2 mechanism. The increase in the thiolysis rate constant could be assigned to the $Ge(OEt)_4$ concentration change. From the similarities of the concentration−time curves obtained for low and high H_2S concentrations, it seems that both sol−gel processes occurred by slow thiolysis and fast condensations.

Conclusions

The mechanistic study of the sol−gel processing of GeS_2 from $Ge(OEt)_4$ and H_2S in toluene solution confirms that the reaction occurs in three suggested steps: thiolysis, the hydrogen sulfide-forming condensation and the alcohol-forming condensation. The intermediate germanium mercaptide formed during thiolysis is a stable product identified in the dry gel. The reaction conditions, concentration of reactants, and their ratio caused the simplification of the proposed mechanism. The reaction occurs by three suggested steps when the molar ratio of $Ge(OEt)_4$ and H_2S is 1.2:1. However, for the ratio 1:9 it simplifies the mechanism only to thiolysis and the alcohol-forming condensation.

Regardless of the reaction conditions, thiolysis is a slow step and condensations are fast. The thiolysis rate increases ~2 times when the concentration of $Ge(OEt)_4$ changes from 0.044 to 0.264 M.

Dependence of the reaction rate constants on temperature is in good agreement with the Arrhenius law and the transition-state theory in the observed temperature range (30 °C to 50 °C). The thiolysis activation energies obtained for two different concentrations of $Ge(OEt)_4$ are similar indicating rapture and formation of the same bonds.

The negative entropy, indicative of association of two molecules in the transition state, confirms that thiolysis and condensations occur by an S_N2 mechanism. Moreover, the second-order reaction obtained for thiolysis and condensations regardless of the conditions is in agreement with these data.

Calculated activation free energies $\Delta G^{\ddagger}$ demonstrate that the rate-determining step is thiolysis. The same conclusion is reached from the experimentally determined reaction rate constants.

Acknowledgment. The authors are grateful to CANMET, Western Research Centre, for financial support of this work.

References and Notes

(1) Matijević, E. *Chem. Mater.* **1993**, *5*, 412.

(2) Pierre, A. C. *Introduction to sol−gel processing*; Septima: Paris, 1992; Chapter 2.

(3) Strelko, V. *Kolloidn. Zh.* **1970**, *32*, 430.

(4) McNeil, K. J.; DiCaprio, J. A.; Walsh, D. A.; Pratt, R. F. *J. Am. Chem. Soc.* **1980**, *102*, 1859.

(5) Assink, R. A.; Kay, B. D. In *Better Ceramics through Chemistry*; Brinker, C. J., Clark, D. E., Ulrich, D. R., Eds.; Elsevier Science: Amsterdam, 1984; p 301.

(6) Assink, R. A.; Kay, B. D. *J. Non-Cryst. Solids* **1988**, *99*, 359.

(7) Assink, R. A.; Kay, B. D. *J. Non-Cryst. Solids* **1988**, *104*, 112.

(8) Assink, R. A.; Kay, B. D. *J. Non-Cryst. Solids* **1988**, *107*, 35.

(9) Doughty, D. H.; Assink, R. A.; Kay, B. D. *In Silicon-based polymer science*; Zeigler, J. M., Fearon, F. W., Eds.; American Chemical Society: Washington, DC, 1990; p 241.

(10) Pouxviel, J. C.; Boilot, J. P.; Beloeil, J. C.; Lallemand, J. Y. *J. Non-Cryst. Solids* **1987**, *89*, 345.

(11) Pouxviel, J. C.; Boilot, J. P. *J. Non-Cryst. Solids* **1987**, *94*, 374.

(12) Artaki, I.; Sinha, S.; Irwin, A. D.; Jonas, J. *J. Non-Cryst. Solids* **1985**, *72*, 391.

(13) Ro, J. C.; Chung, I. J. *J. Non-Cryst. Solids* **1989**, *110*, 26.

(14) Kline, A. A.; Mullins, M. E.; Cornilsen, B. C. *J. Am. Ceram. Soc.* **1991**, *74*, 2559.

(15) Kline, A. A.; Rogers, T. N.; Mullins, M. E.; Cornilsen, B. C.; Sokolov, Lj. M. *J. Sol−Gel Sci. Technol.* **1994**, *2*, 269.

(16) Sanchez, J.; Mary, R.; McCormick, A. In *Better Ceramics through Chemistry*; Zelinski, B. J., Brinker, J. C., Clark, D. E., Urlich, D. R., Eds.; Matererials Research Society: Pittsburgh, PA, 1990; 180, p 263.

(17) Liu, J.; Kim, S. D. *J. Polym. Sci., Part B: Polym. Phys.* **1996**, *34*, 131.

(18) Stanić, V.; Mikula, R. J.; Pierre, A. C.; Etsell, T. H. *Electrochem. Acta* **1998**, *43*, 2639.

(19) Melling, P. J. *Am. Ceram. Soc. Bull.* **1984**, *63*, 1427.

(20) Stanić, V.; Mikula, R. J.; Pierre, A. C.; Etsell, T. H. *J. Mater. Res.* **1996**, *11*, 364.

(21) Lewis, E. S. *Investigation of rates and mechanisms of reactions*, 3rd ed.; John Wiley & Sons: New York, 1974; Chapter 2.

(22) Laidler, K. J. *Chemical kinetics*, 2nd ed.; McGraw-Hill Book Company: New York, 1965; Chapter 3.

(23) Espenson, J. H. *Chemical kinetics and reaction mechanisms*; McGraw-Hill Book Company: New York, 1981; Chapter 5.

(24) Veljković, S. *Chemical kinetics*; Gradjevinska knjiga: Beograd, 1969; Chapter 5.

(25) Langford, C. H.; Gray, H. B. *Ligand substitution process*; W. A. Benjamin Inc.: New York, 1966.